*International Journal of Research in Engineering and Science (IJRES)*
*ISSN (Online): 2320-9364, ISSN (Print): 2320-9356*
*www.ijres.org Volume 10 Issue 4 ǁ 2022 ǁ PP. 71-78*

# Performance evaluation of an innovative configuration of the desiccant dehumidifier with a silica gel-based composite with $Al_2O_3$ nanoparticles for adsorption air conditioners

A. E. Kabeel, Mohamed Fathy Nada, Mohamed Abdelgaied
*Mechanical Power Engineering Department, Faculty of Engineering, Tanta University, Egypt*

***Abstract***
*The present experimental study aims to innovate a new design of desiccant dehumidifier that operated with high efficiency, in order to improve the performance of desiccant air conditioners to achieve the thermal comfort conditions with the lowest power consumption rates. This was done by constructing, designing, and testing an innovative configuration of the desiccant dehumidifier with a silica gel-based composite with $Al_2O_3$ nanoparticles for adsorption air conditioners. A proposed configuration consists from two innovative configurations of the desiccant dehumidifier, air blower, and electrical air heater. The experimental results showed that use the innovative configuration of the desiccant dehumidifier improve the dehumidification process, the average the moisture removed capacity reached 8.7 $g_w/kg_{\,dry\,air}$. Also, the average dehumidification coefficient of performance reached 0.402, 0.42, and 0.403 for reactivation air temperature 75 $^oC$, 80 $^oC$, and 85 $^oC$, respectively. These results presented that the highest dehumidification coefficient of performance was achieved at a regeneration air temperature of 80 $^oC$. Moreover; by adding the $Al_2O_3$ nanoparticles to the silica gel the cycle time for reactivation is reduced to 35 min, this will reduce the power consumption rates for reactivating the desiccant dehumidifier.*

***Keywords:*** *Desiccant dehumidifier; Silica gel; $Al_2O_3$ nanoparticles; Cut-segmental silica-gel baffles; Experimental study; Performance Improvement.*

---

Date of Submission: 04-04-2022 Date of acceptance: 19-04-2022

---

## I. Introduction

Most hot and humid regions suffer from rising temperatures. To overcome the problem of temperature rise, it is necessary to adapt the air to achieve the conditions of thermal comfort and this is through the use of desiccant air conditioners, which are characterized by not producing polluting gases such as chlorofluorocarbons produced by traditional vapor-compression refrigeration air conditioning systems. To reduce the consumption of electric power in air conditioning systems, a hybrid system of desiccant air conditioning was used.

The desiccant air conditioning systems represents one of the most important air conditioning systems which are characterized by not producing polluting gases such as chlorofluorocarbons produced by traditional air conditioning systems. The performance of a desiccant air conditioner has been studied numerically by [1-5] studied numerically the impacts of two-stage rotary desiccant on the performance of desiccant A/C. Ge et al. [6] experimentally conducted the influences of two-stage rotary desiccant on A/C performance. Bourdoukan et al. [7] compare recirculation and ventilation cycles on the desiccant air conditioner. Pandelidis et al. [8] studied a hybrid A/C performance with various types of indirect evaporative coolers. Gadalla and Saghafifar [9] conducted the impact of maisotsenko cooler as a pre-cooling on a desiccant A/C performance. The hybrid system contains three maisotsenko coolers, two desiccant wheels, a heat exchanger, and solar collectors. Elzahzby et al. [10, 11] studied the impact of a six-stage inter-cooler on the thermal performance of desiccant A/C. Kabeel et al. [12] conducted the impact of IDEC with baffles as a pre-cooling unity on the performance of hybrid A/C. Kabeel and Abdelgaied [13] conducted the impact of PCM on the performance of desiccant A/C assisted by solar energy. Kabeel and Abdelgaied [14] conducted the influence of internal baffles on the performance of indirect evaporative cooler (IDEC). The influence of IDEC with internal baffles as a pre-cooling unit on the performance of evaporative condenser was studied by [15].

Olmuş et al. [16] numerically studied the behavior of the new solid desiccant air-conditioning system configuration integrated with direct and dew-point indirect evaporative coolers and photovoltaic/thermal panels. Gao et al. [17] presented a comprehensive review about the different improvement techniques which aimed to improve the performance of solid desiccant air conditioners. Ali et al. [18] utilized the chilled water-cooling coil

heat exchanger integrated with the absorption chiller as sensible cooling unit to improve the performance of solid desiccant air conditioning. The experimental results concluded that the supply air temperature for the integrated system reduced to 15.2 ◦C compared to 24.6 ◦C achieved by conventional desiccant system. Abdelgaied et al. [19] experimentally studied the overall performance of solid desiccant air conditioners integrated with the humidification-dehumidification desalination unit. These systems aimed to achieve thermal comfort conditions and produce pure water with lost power consumption rates. Kabeel and Abdelgaied [20] experimentally studied the behavior of new configuration of the desiccant dehumidifier with cut-segmental silica-gel baffles and for air conditioning integrated with humidification-dehumidification desalination system.
The present study aims to overcome the problems of human thermal comfort issues facing hot and humid regions. To investigate this idea, an innovative configuration of the desiccant dehumidifier with a silica gel-based composite with Al2O3 nanoparticles for desiccant air conditioning was constructed and tested at Tanta University, Egypt. A proposed configuration consists of two innovative configurations of the desiccant dehumidifier, air blower, and electric air heater. The proposed innovative configuration of the desiccant dehumidifier aimed to of added the Al2O3 nanoparticles to the silica gel as composite desiccant materials to achieve the thermal comfort condition with lost power consumption rates. To find the characteristics and evaluate the feasibility and energy-saving potential of this new configuration of the suggested device, the cycle time, moisture removal capacity, relative moisture removal capacity, and dehumidification coefficient of the performance was experimentally evaluated.

## II. Experimental Set-up

The present experimental work aims to illustrate the influences of added the $Al_2O_3$ nanoparticles to the silica gel as a composite desiccant materials on the performance of an innovative configuration of the desiccant dehumidifier. Figs. 1 and 2 show a schematic diagram and photograph of an innovative configuration of the desiccant dehumidifier with a silica gel-based composite with $Al_2O_3$ nanoparticles. A proposed configuration consists from two innovative configurations of the desiccant dehumidifier, air blower, and electrical air heater. An innovative configuration of the desiccant dehumidifier consist form square cross-section channel made from galvanized steel 1.5 mm thick has dimensions of 20 cm × 20 cm × 90 cm length. This channel contains ten cut-segmental baffles made from the silica-gel-based composite with $Al_2O_3$ nanoparticles, the dimension of each baffle are 20 cm × 15 cm × 2.5 cm thick. The specifications of the silica gel utilized in thus work are (particle beads size 1-3 mm, density 761 kg/m$^3$, specific heat 921 J/kg K, and porosity 0.43). Also, the specifications of $Al_2O_3$ nanoparticles utilized in this work are (average particles size 3-5 nm, thermal conductivity 38.5 W/m K, specific heat capacity 880 J/kg K, and the density 3.89 g/cm$^3$). The total mass of silica gel for each desiccant dehumidifier is 5.7 kg and the total mass of $Al_2O_3$ nanoparticles added to the silica gel for each desiccant dehumidifier is 285 g with the weight ratio 5%. The cooling water passes through a four straight copper tube 1.25 inches diameter and 100 cm length for each channel as shown in Fig. 3. All outside surfaces of desiccant dehumidifier are insulated by 50 mm glass wool blanket (coefficient of thermal conductivity 0.041 W/m K) to minimize the heat transfer between desiccant dehumidifier and its surrounding. The proposed system contains two centrifugal air fans 375 W.

The paths of process air and reactivation air of the suggested innovative configuration of the desiccant dehumidifier on the psychometric chart are shown in Fig. 4.

For two the innovative configurations of the desiccant dehumidifier, one for reactivation air and the other for processing air, alternately were alternating between them. The process air is cooled and dehumidified in the first desiccant dehumidifier from state points 1-2, as well as the reactivation air is first heated in the electrical air heater from the state point 1-3, after that the reactivation air cooled and humidified in the second desiccant dehumidifier from state points 3-4, as shown in Fig. 4.

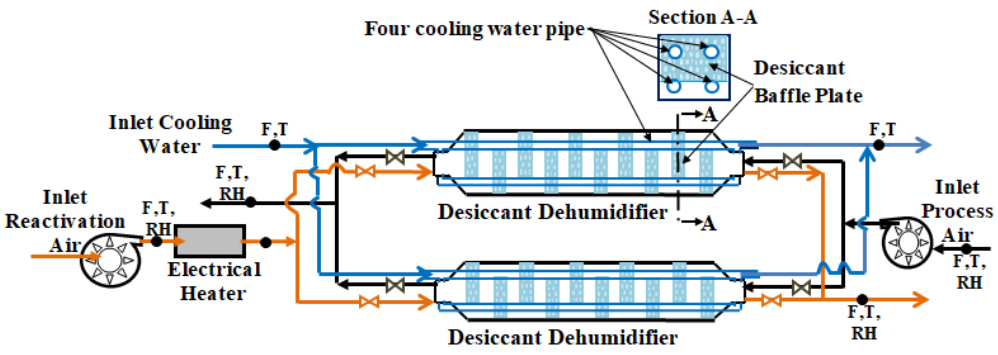


Fig. 1 Schematic diagram of an innovative configuration of the desiccant dehumidifier with a silica gel-based composite with $Al_2O_3$ nanoparticles

Fig. 2 A photograph of the experimental set-up

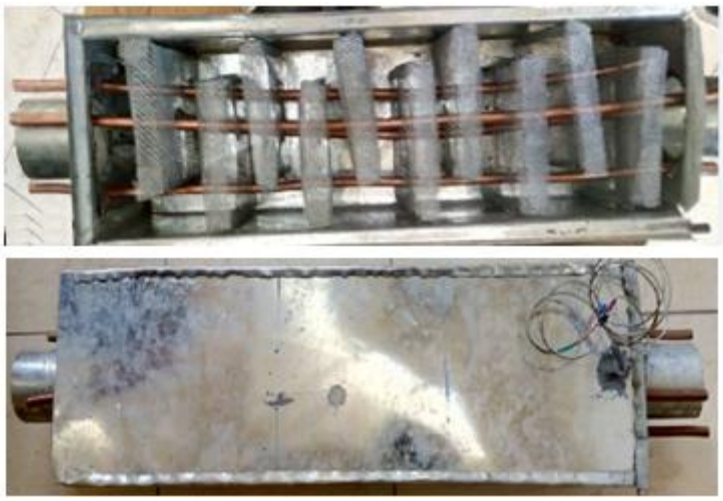

Fig. 3 A photographic of an innovative configuration of the desiccant dehumidifier

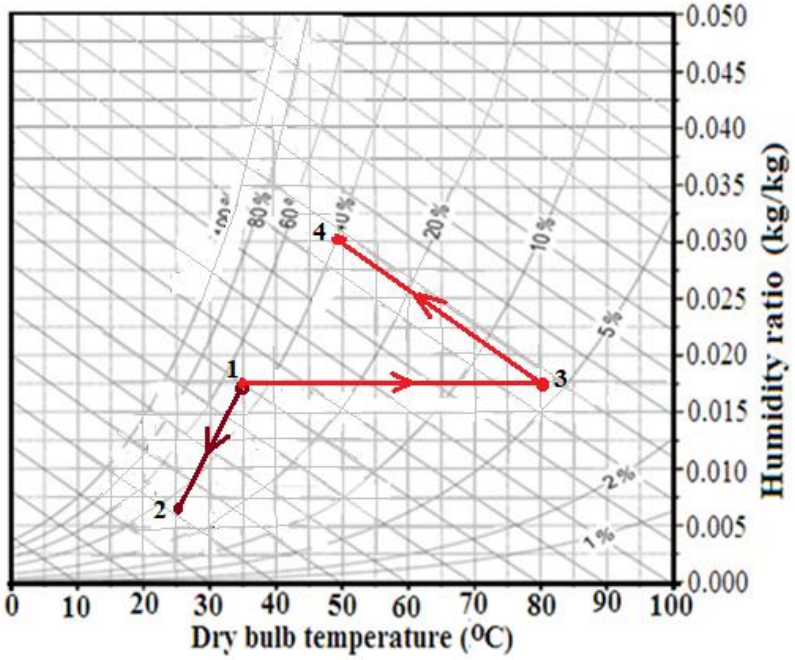


Fig. 4 Paths of process air and reactivation air on the psychometric chart

## III. Measuring instruments and errors analysis

To evaluate the performance of an innovative configuration of the desiccant dehumidifier with a silica gel-based composite with $Al_2O_3$ nanoparticles for adsorption air conditioners, the air temperature, relative humidity, and discharge of (reactivation air, process air, cooling water) are measured along the test days. The specifications of all measuring devices utilized to record the experimental data are presented in Table 1.

Table 1 Specifications of all measuring devices

| Measuring Device | Accuracy | Range | % Error |
|---|---|---|---|
| Relative humidity sensor | ± 1% RH | 0–100% RH | 1.95 |
| Digital temperature sensor | ± 0.5 °C | 0–125 °C | 1.28 |
| Air flow meter | ± 0.1 m $s^{-1}$ | 0.0–10 m $s^{-1}$ | 2.8 |
| Water flow meter | ± 0.05 l $min^{-1}$ | 1–7 l $min^{-1}$ | 1. 05 |

## IV. System performance

The main function of a desiccant dehumidifier is to remove water vapor from the process air that passes through it. Therefore, the first group of performance indicators represents the dehumidification capacity of the desiccant dehumidifier. The moisture removal capacity MR is defined as:

$$MR = \omega_{p,out} - \omega_{p,in} \quad (1)$$

where $\omega_{p,out}$ and $\omega_{p,in}$ are output and input humidity ratio of process air of desiccant dehumidifier, respectively.

Relative moisture removal is defined as the ratio between the moisture removal capacities MR to the humidity ratio of process air inlet to the desiccant dehumidifier $\omega_{p,in}$ as follows:

$$\text{Relative moisture removal} = \frac{MR}{\omega_{p,in}} \quad (2)$$

Dehumidification coefficient of performance DCOP of the desiccant dehumidifier, which is defined as the ratio of the latent heat which is contained in the adsorbed moisture and the reactivation heat used for reactivation air which calculated as follows:

$$DCOP = \frac{\dot{m}_{p,air} \times MR \times h_{fg}}{\dot{m}_{r,air} \times C_{p,air} \times (T_{r,out} - T_{r,in})} \quad (3)$$

## V. Experimental Results

Along the test days, the discharge of the process air and reactivation air remains constant at 120 $m^3$/h and the cooling water flow rate through the desiccant dehumidifier remains constant at 4 liter/min.

In the proposed system, a pair of an innovative configuration of the desiccant dehumidifier with a silica gel-based composite with $Al_2O_3$ nanoparticles runs at the same time parallel in two different modes. If the first desiccant dehumidifier is in cooling with dehumidification mode then second desiccant dehumidifier will be in reactivation mode and after reaching the saturation state, the second desiccant dehumidifier will be in cooling with dehumidification mode and first desiccant dehumidifier will be in reactivation mode. Fig. 5 shows the influences of adding the Al2O3 nanoparticles to the silica gel as composite desiccant materials on the amount of moisture removal capacity within the desiccant dehumidifier. As shown in Fig. 5 the cycle time for the first and second desiccant dehumidifier with only silica gel are 40 min, but for adding the $Al_2O_3$ nanoparticles to the silica gel the cycle time for reactivation is reduced to 35 min. this is mainly because of the effect of thermal energy storage in $Al_2O_3$ nanoparticles. This will be reduced the power consumption rates for reactivating the desiccant dehumidifier.

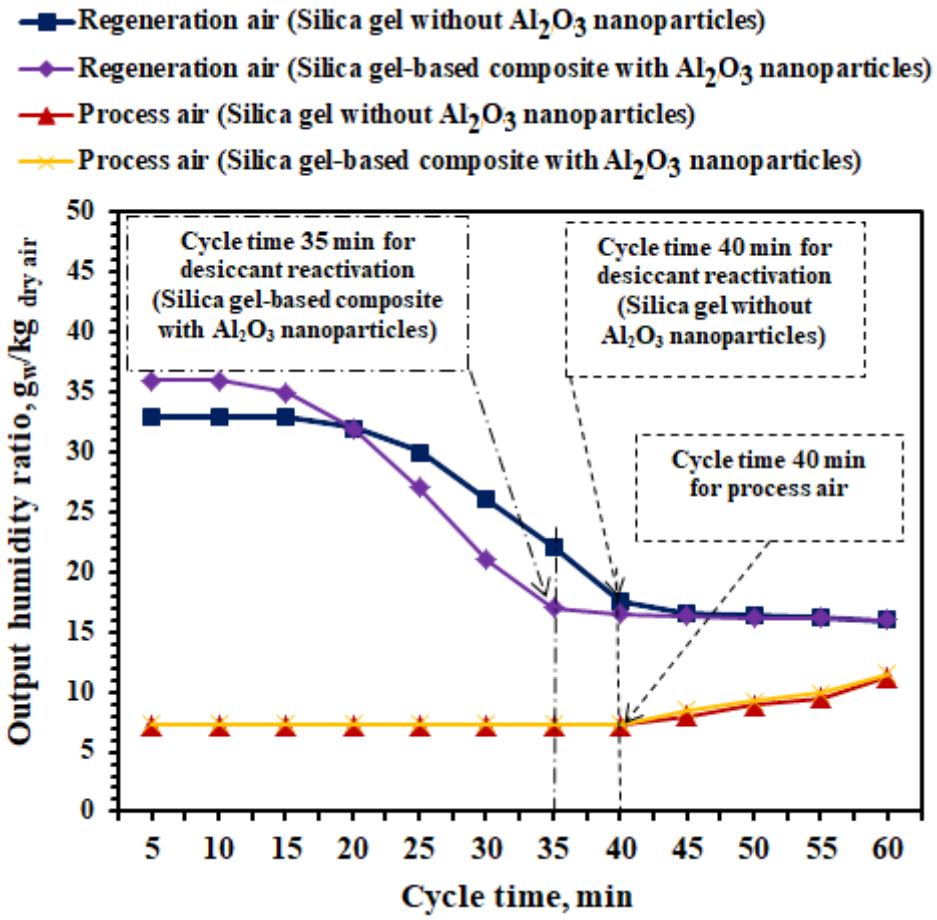


Fig. 5 Cycle time of a pair of an innovative configuration of the desiccant dehumidifier.

The variation of ambient air temperature and the relative humidity of ambient air with time during the period from 9:00 am to 6:00 pm are shown in Fig. 6. As shown in this figure, the ambient air temperature varies between 31.5-36 oC, 32-36.5 oC, and 32-36 oC, for the first, second, and third test days, respectively. Also, the relative humidity of ambient air varies between 44-54%, 44-53%, and 45-53% for the first, second, and third test days, respectively, during the period from 9:00 am to 6:00 pm.

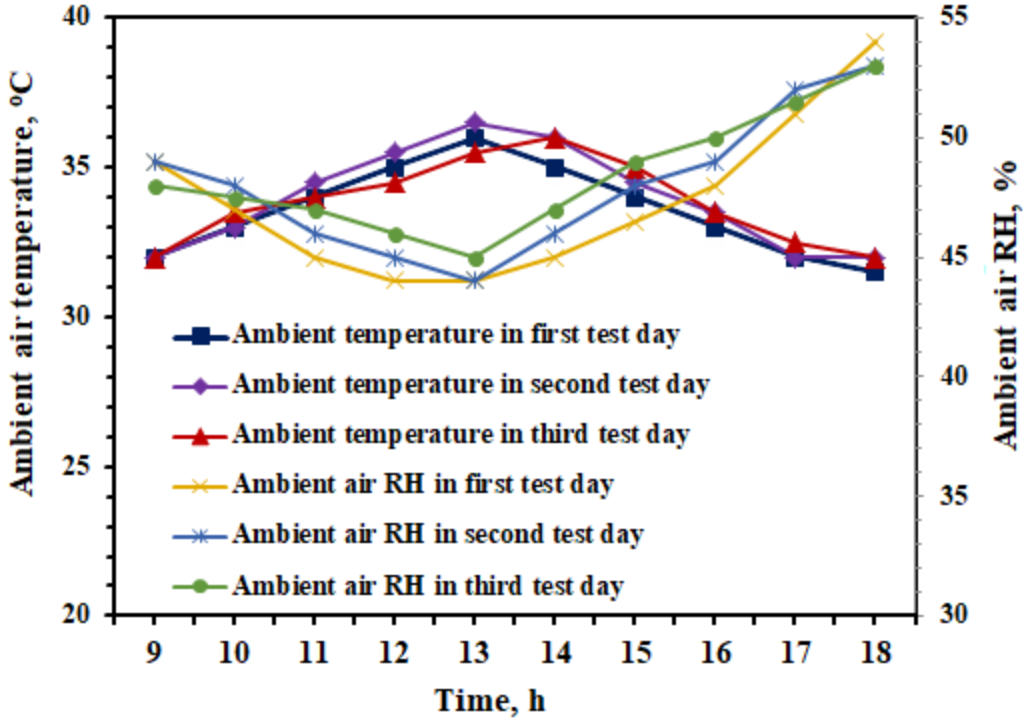


Fig. 6 Variations of ambient air temperature relative humidity during the three test days starting from 9:00 am till 6:00 pm.

Fig. 7 shows the variation of the moisture removed capacity from the process air during the desiccant dehumidifier starting from 9:00 am till 6:00 pm at reactivation air temperature 75 °C, 80 °C, and 85 °C. As shown in Fig. 7, the moisture removed capacity changes between 6.3-7.8 $g_w/kg_{\text{dry air}}$, 7.5-8.8 $g_w/kg_{\text{dry air}}$, and 8.2-9.4 $g_w/kg_{\text{dry air}}$ for reactivation air temperature 75 °C, 80 °C, and 85 °C, respectively. Also, as shown in Fig. 8 the relative moisture removal capacity changes between 0.38-0.51, 0.45-0.58, and 0.49-0.62 for reactivation air temperature 75 °C, 80 °C, and 85 °C, respectively. The average relative moisture removal capacity reached 0.45, 0.52, and 0.56 for reactivation air temperature 75 °C, 80 °C, and 85 °C, respectively. These results presented that the average relative moisture removal capacity improved by a rate reached 0.11 for increase the reactivation air temperature from 75 °C to 85 °C. These results presented that the moisture removal capacity increases with an increase in the reactivation air inlet temperature due to the desiccant dehumidifier being better regenerated.

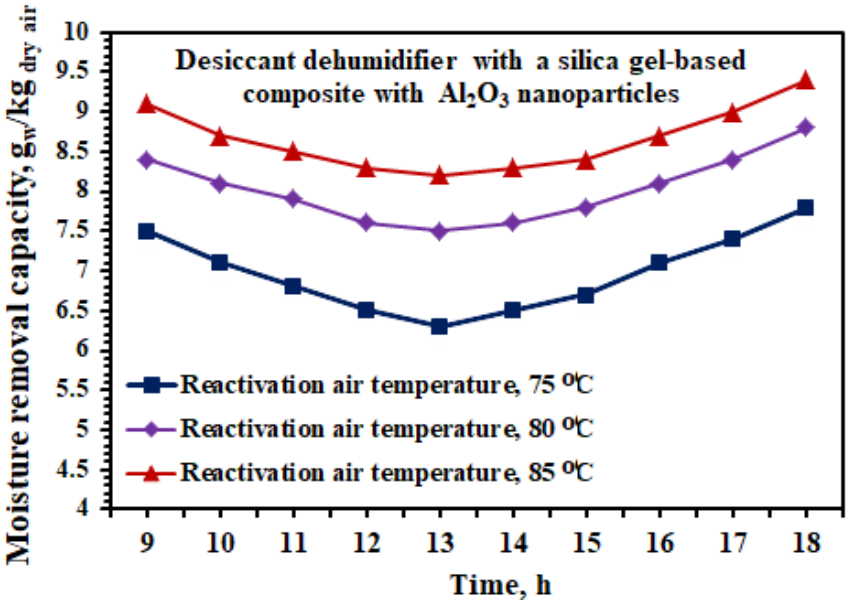


Fig. 7 Variation of the moisture removed capacity for an innovative configuration of the desiccant dehumidifier with a silica gel-based composite with $Al_2O_3$ nanoparticles starting from 9:00 am till 6:00 pm.

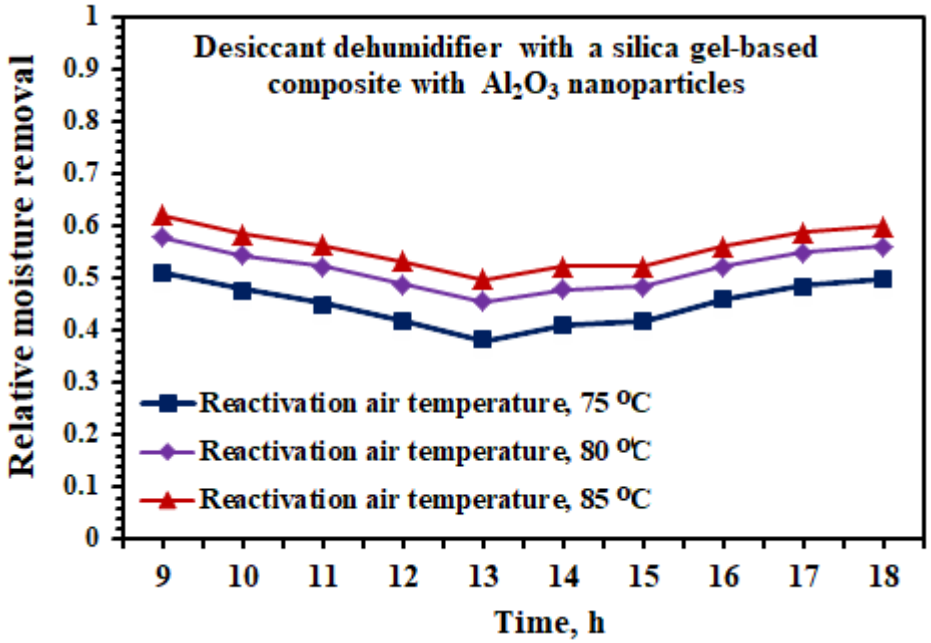


Fig. 8 Variation of the relative moisture removed capacity for an innovative configuration of the desiccant dehumidifier with a silica gel-based composite with $Al_2O_3$ nanoparticles starting from 9:00 am till 6:00 pm.

Fig. 9 shows the variation of dehumidification coefficient of performance DCOP of the desiccant dehumidifier starting from 9:00 am till 6:00 pm at reactivation air temperature 75 °C, 80 °C, and 85 °C. Also, as shown in Fig. 9 the dehumidification coefficient of performance changes between 0.39-0.43, 0.41-0.44, and 0.4-0.42 for reactivation air temperature 75 °C, 80 °C, and 85 °C, respectively. The average dehumidification coefficient of performance reached 0.402, 0.42, and 0.403 for reactivation air temperature 75 °C, 80 °C, and 85 °C, respectively. These results presented that the highest dehumidification coefficient of performance was achieved at a regeneration air temperature of 80 °C. After that with an increase in the regeneration air temperature, the dehumidification coefficient of performance will be decreased.

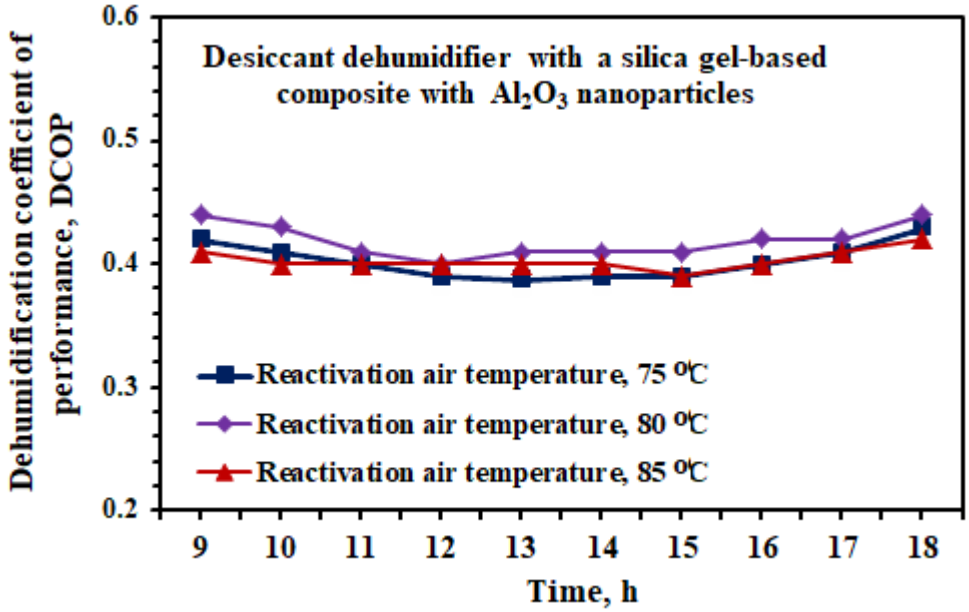


Fig. 9 Variation of DCOP for an innovative configuration of the desiccant dehumidifier with a silica gel-based composite with $Al_2O_3$ nanoparticles starting from 9:00 am till 6:00 pm.

## VI. Conclusions

In this study, the performance of an innovative configuration of the desiccant dehumidifier with a silica gel-based composite with $Al_2O_3$ nanoparticles for adsorption air conditioners was experimentally investigated. The aims of a suggested innovative configuration of the desiccant dehumidifier are to achieve the thermal comfort condition with the lowest power consumption rates. The main experimental results can be drawn as follows:

- The cycle time required for reactivation of the desiccant dehumidifier was reduced to 35 min by adding the $Al_2O_3$ nanoparticles to the silica gel. This will be reduced the power consumption rates for reactivating the desiccant dehumidifier.
- The moisture removed capacity changes between 6.3-7.8 $g_w/kg_{\text{ dry air}}$, 7.5-8.8 $g_w/kg_{\text{ dry air}}$, and 8.2-9.4 $g_w/kg_{\text{ dry air}}$ for reactivation air temperature 75 $^oC$, 80 $^oC$, and 85 $^oC$, respectively.
- The average relative moisture removal capacity reached 0.45, 0.52, and 0.56 for reactivation air temperature 75 $^oC$, 80 $^oC$, and 85 $^oC$, respectively.
- The average improvement in relative moisture removal capacity reached 0.11 for increase the reactivation air temperature from 75 $^oC$ to 85 $^oC$.
- The average dehumidification coefficient of performance reached 0.402, 0.42, and 0.403 for reactivation air temperature 75 $^oC$, 80 $^oC$, and 85 $^oC$, respectively.
- The highest dehumidification coefficient of performance was achieved at a regeneration air temperature of 80 $^oC$.

## References


[1]. Zheng W., Worek W.M., Novesel D., Performance optimization of rotary dehumidifiers. ASME Journal of Solar Energy Engineering 117 (1995); 40–44.

[2]. Zhang X.J., Dai Y.J., A simulation study of heat and mass transfer in a honeycombed rotary desiccant dehumidifier, Applied Thermal Engineering 23 (8), (2003); 989–1003.

[3]. Chung J. D., Dae-Young Lee, Effect of desiccant isotherm on the performance of desiccant wheel. International journal of refrigeration 32 (2009) 720–726.

[4]. Ge T.S., Ziegler F., Wang R.Z., A mathematical model for predicting the performance of a compound desiccant wheel (A model of compound desiccant wheel). Applied Thermal Engineering 30 (2010); 1005–1015.

[5]. Meckler G., Two-stage desiccant dehumidification in commercial building HVAC systems, ASHRAE Trans 95(2) (1989); 1116–1123.

[6]. Ge TS, Dai YJ, Wang RZ, Li Y., Experimental investigation on a one-rotor two stage rotary desiccant cooling system. Energy 33(12) (2008); 1807–1815.

[7]. Bourdoukan P, Wurtz E, Joubert P., Comparison between the conventional and recirculation modes in desiccant cooling cycles and deriving critical efficiencies of components. Energy 35(2) (2010); 1057–1067.

[8]. Pandelidis Demis, Anisimov Sergey, Worek M.William, Drag Paweł, Comparison of desiccant air conditioning systems with different indirect evaporative air coolers, Energy Conversion and Management 117 (2016); 375–392.

[9]. Gadalla Mohamed, Saghafifar Mohammad, Performance assessment and transient optimization of air precooling in multi-stage solid desiccant air conditioning systems, Energy Conversion and Management 119 (2016); 187–202.

[10]. Elzahzby Ali M., Kabeel A.E., Bassuoni M.M., Mohamed Abdelgaied, Effect of inter-cooling on the performance and economics of a solar energy assisted hybrid air conditioning system with six stages one-rotor desiccant wheel, Energy Conversion and Management 78 (2014); 882-896.

[11]. Elzahzby Ali M., Kabeel A.E., Bassuoni M.M., Mohamed Abdelgaied, A mathematical model for predicting the performance of the solar energy assisted hybrid air conditioning system, with one-rotor six-stage rotary desiccant cooling system, Energy Conversion and Management 77 (2014); 129–142.

[12]. Kabeel A.E., Mohamed Abdelgaied, Ravishankar Sathyamurthy, T. Arunkumar, Performance improvement of a hybrid air conditioning system using the indirect evaporative cooler with internal baffles as a pre-cooling unit, Alexandria Engineering Journal 56(4) (2017); 395-403.

[13]. Kabeel A.E., Mohamed Abdelgaied, Solar energy assisted desiccant air conditioning system with PCM as a thermal storage medium, Renewable Energy 122 (2018); 632-642.

[14]. Kabeel A.E., Abdelgaied Mohamed, Numerical and experimental investigation of a novel configuration of indirect evaporative cooler with internal baffles, Energy Conversion and Management 126 (2016); 526–536.

[15]. Kabeel A.E., Bassuoni M.M., Abdelgaied Mohamed, Experimental study of a novel integrated system of indirect evaporative cooler with internal baffles and evaporative condenser, Energy Conversion and Management 138 (2017); 518–525.

[16]. Olmuş U., Güzelel Y.E., Pınar E, Özbek A., Büyükalaca O., Performance assessment of a desiccant air-conditioning system combined with dew-point indirect evaporative cooler and PV/T, Solar Energy 231 (2022) 566-577.

[17]. Gao D.C., Sun Y.J., Ma Z., Ren H., A review on integration and design of desiccant air-conditioning systems for overall performance improvements, Renewable and Sustainable Energy Reviews 141 (2021) 110809.

[18]. Ali M., Habib M. F., Sheikh N.A., Akhter J., Gilani S.I.H., Experimental investigation of an integrated absorption- solid desiccant air conditioning system, Applied Thermal Engineering 203 (2022) 117912.

[19]. Abdelgaied M., Kabeel A.E., Zakaria Y., Performance improvement of desiccant air conditioner coupled with humidification-dehumidification desalination unit using solar reheating of regeneration air, Energy Conversion and Management 198 (2019) 111808.

[20]. Kabeel A.E., Abdelgaied M., A new configuration of the desiccant dehumidifier with cut-segmental silica-gel baffles and water cooling for air conditioning coupled with HDH desalination system, International Journal of Refrigeration 103 (2019) 155-162.